Photoinduced phase transitions in VO_2: visualizing the time-dependent crystal potential using ultrafast electron diffraction data

Laurent P. René de Cotret[1], Martin R. Otto[1], N. Émond[3], M. Chakker[3] and Bradley J. Siwick[1,2]

[1]Department of Physics, Center for the Physics of Materials, McGill University, Montréal, Québec, Canada
[2]Department of Chemistry, McGill University, Montréal, Québec, Canada
[3]Institut national de recherche scientifique, Varennes, Québec, Canada

McGill
Siwick Research Group
Departments of Physics and Chemistry
www.physics.mcgill.ca/siwicklab

Motivation

Vanadium dioxide is notable for exhibiting several low-T insulating phases and having a very well studied insulator-metal transition (IMT) at ~68°C that is associated with a crystallographic change from monoclinic semiconductor (M1) to rutile metal (R). The nature of the IMT has been the subject of vigorous debate since 1959, with recent work suggesting that the electronic properties of both phases emerge from a complex interaction of lattice, orbital and charge degrees of freedom.

Using a combination of ultrafast electron diffraction (UED) and broadband spectroscopy, we have recently demonstrated that photoexcitation of monoclinic vanadium dioxide crystals below a threshold fluence induces a transition to a metastable state with monoclinic crystallography, but metal-like optical/electronic properties [1]. This long-lived metallic phase appears to have no equilibrium analog. The development of new ultrafast electron powder diffraction analysis tools in order to provide a detailed structural characterization of such photoinduced phases is the subject of this poster.

Ultrafast electron diffraction

The ultrafast electron diffraction (UED) instrument in the Siwick laboratory probes samples with short (~100fs) bunches of ~100 keV electrons. The setup is synchronized with an oscillator that drives both a laser system and a radio-frequency cavity. This cavity is used to counteract the Coulomb repulsion that stretches the electron bunches. Therefore, the RF-UED system is not subject to the historical trade-off between a high signal-to-noise ratio (electron pulse fluence) and time-resolution (short electron bunches) [2].

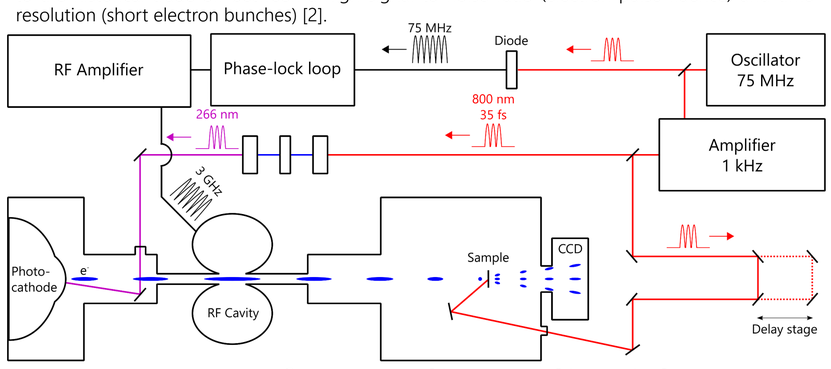

UED of vanadium dioxide

The structure of the VO_2 unit cell *during* the photoinduced IMT was observed over a broad range of pump fluence using ultrafast electron powder diffraction. This study revealed qualitatively distinct 'fast' and 'slow' structural reorganizations. The fast change is associated with a transition to the rutile phase, while the slow change is associated with a 1D reorganization that preserves monoclinic crystallography [1]. At pump fluences below ~9 mJ/cm² only the slow dynamics are observed.

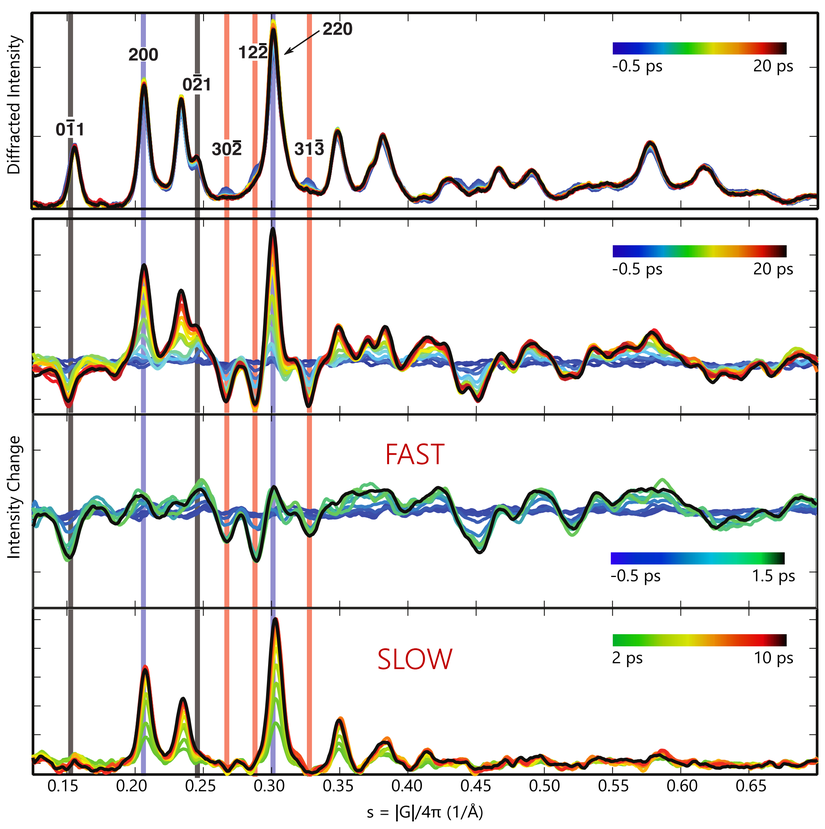

Above: time-resolved radially-averaged polycrystalline diffraction pattern. **Middle**: radially-averaged diffraction changes for various time scales. Red overlays corresponds to peaks allowed in a monoclinic but not rutile. Blue overlays indicate peaks that appear in both equilibrium phases. Grey overlays designates structural changes orthogonal to $\mathbf{c}_R$. **Bottom**: diffracted intensity changes for 2 ps – 10 ps.

Key step: baseline-removal

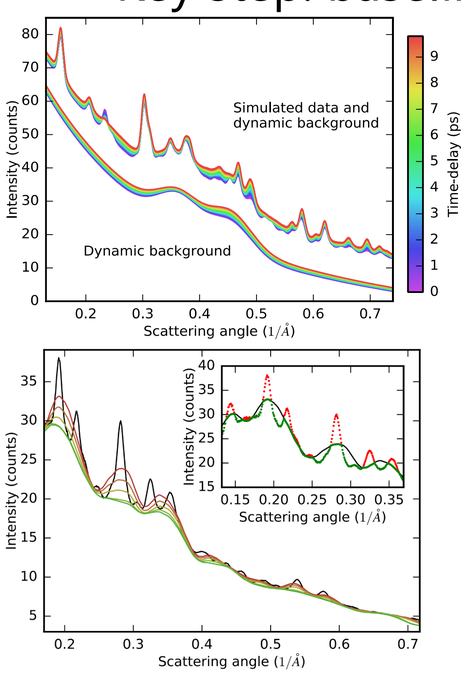

Reliably separating the sample dynamics from the background is a key processing step in UEPD. This is difficult in the current circumstance because of the many overlapping peaks and lack of regions that can be considered exclusively background.
Interpolation and curve-fitting are only reliable in certains cases. Fourier methods also fail because of the frequency-domain overlap between the peaks and background. Wavelet transforms are able to decompose signals into local frequency components, without artifacts associated with the windowed Fourier transform.

An iterative algorithm that recursively approximates the baseline can be formulated using the dual-tree complex wavelet transform [4], which can then be subtracted from the diffracted intensities at each time-point. The performance of this routine depends on the chosen wavelet family.

Top: simulated ultrafast electron powder diffraction dataset of photoinduced phase transition of VO_2 from monoclinic M1 to rutile. The background is given exaggerated dynamics to showcase the power of the algorithm. **Bottom**: effect of iteration on the algorithm. **Inset**: visualization of a single iteration. The signal is decomposed into wavelets, and the narrowest of which are removed (red). The remaining signal (green) is passed to the next iteration.

Baseline-removal II

Applying the algorithm to a simulated dataset with known dynamics, we can determine the error in baseline-determination. While the absolute error can be as high as 2%, the evolution of this error is capped at 1%. This means that time-constants from dynamics can be extracted with very little distortion. The iterative algorithm was tested with dual-tree complex wavelets and real-valued wavelets; the use of the dual-tree complex wavelet transform lowered the absolute error (and it's evolution) by a factor of 2X.

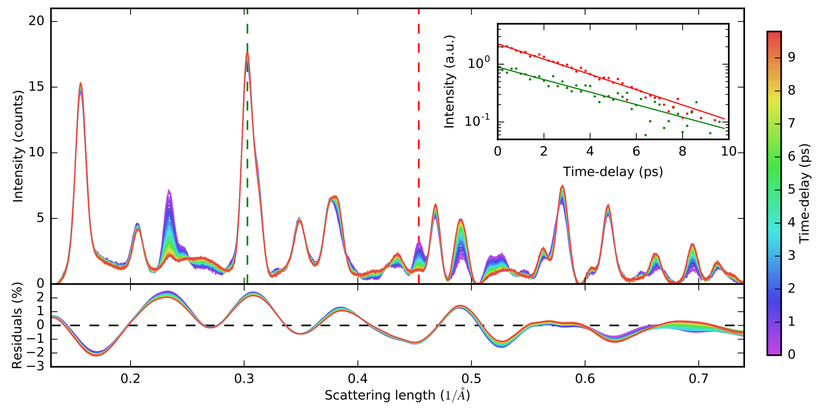

Top: simulated experiment on monoclinic M1 VO2. Dynamic background is exaggerated to showcase the performance of the algorithm. **Bottom**: background-subtracted UEPD dataset using the dual-tree complex wavelet transform. The error evolution over time is capped at 1%, even with non-exponential simulated background dynamics. **Inset**: exponential fit extracted from peaks highlighted by colored (dashed) lines show no distortion from purely exponential.

Electrostatic potential maps

For the case of centrosymmetric crystals, diffraction phases are either 0 or π radians. From structure factor calculations, we can assign phases for each reflection. Then, an inverse Fourier transform can be used on the diffraction data to get the scattering potential map:

$$\phi(\boldsymbol{r}) = \sum_{\{\boldsymbol{G}\}} |S(\boldsymbol{G})|\, e^{i\chi_{\boldsymbol{G}}}\, \cos(\boldsymbol{G}\cdot\boldsymbol{r})$$

for scattering (electrostatic) potential ϕ, real-space position vector $\boldsymbol{r}$, reflections $\{\boldsymbol{G}\}$, and structure factor amplitude $|S(\boldsymbol{G})|$ and phase $\chi_{\boldsymbol{G}}$.

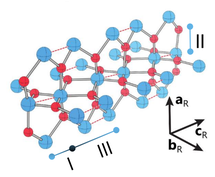

Crystal structure of monoclinic M1 VO_2. Roman numerals indicate prominent peaks in the radial pair-distribution function below.

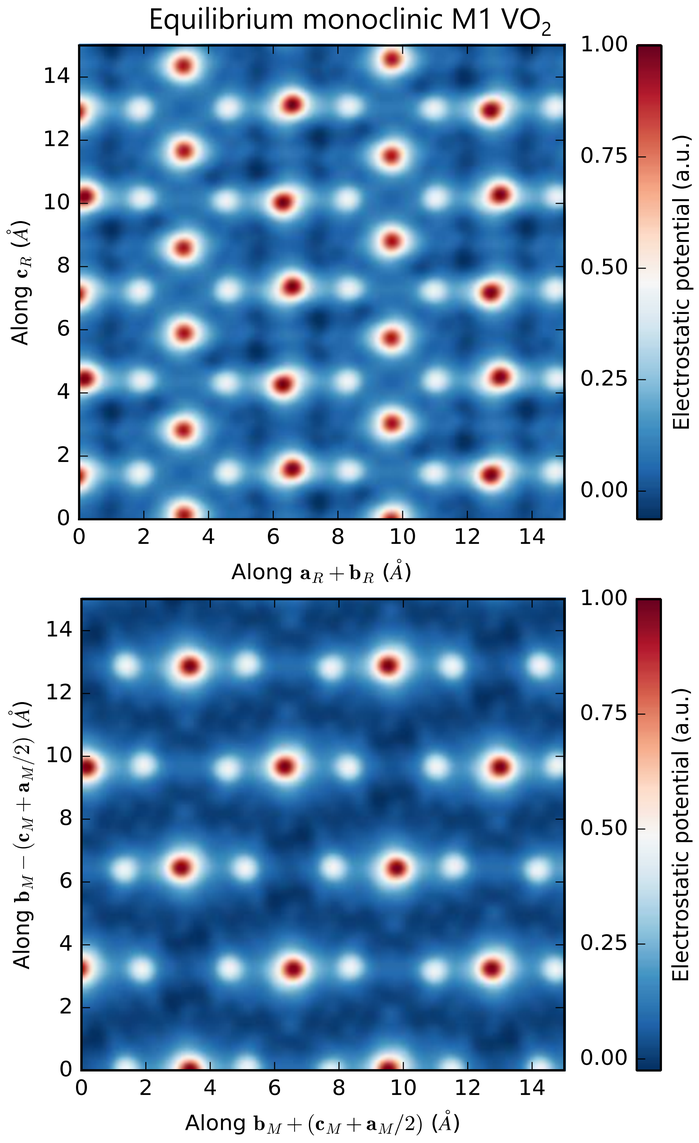

Electrostatic potential of equilibrium, monoclinic VO_2. **Top**: electrostatic potential slice along the rutile c-axis, showcasing the V – V dimers. **Bottom**: electrostatic potential slice perpendicular to the V – V dimers.

We test the validity of the electrostatic potential maps by comparing the radial pair-distribution function (PDF). The PDF can be obtained from the angular average of the (reduced) Patterson function $P(\boldsymbol{r})$ [3]. It is possible to calculate the PDF in two equivalent but separate ways: directly from the diffraction intensity data, and via autocorrelation of the generated electrostatic potential maps.

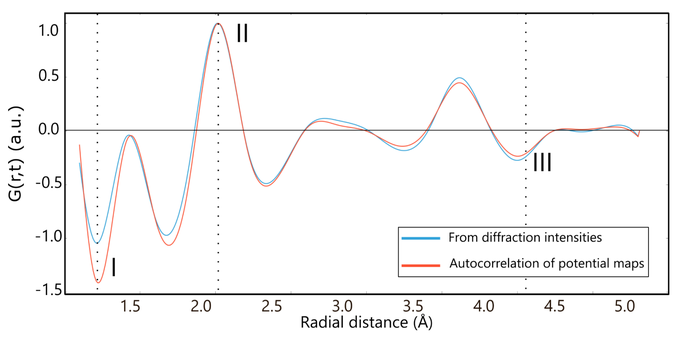

Pair-distribution function comparison between a direct calculation from the equilibrium diffracted intensity data and an autocorrelation of electrostatic potential calculation. Perfect agreement between the two curves signifies that the assumptions in computing the electrostatic potential maps are valid. Roman numerals are echoed by atomic distances in the crystal structure of VO_2 above.

Photoinduced changes

Electrostatic potential maps provide a much richer way to visualize the structure of the material than the radial pair-distribution functions. We generate difference electrostatic potential maps from the UED data in the range {1.5ps – 10ps} to determine a detailed view of the structural changes associated with the transition to the unique nonequilibrium monoclinic metallic phase.

Looking at the plane spanned by $\mathbf{c}_R$ and ($\mathbf{a}_R$ + $\mathbf{b}_R$) allows probing both non-equivalent vanadium positions in the same map. The difference map shows that the electrostatic potential increases at vanadium and oxygen positions and decreases in the 1D charge density waves along $\mathbf{c}_R$ while the tilting and dimerization of the vanadium atoms associated with the monoclinic M1 structure remains.

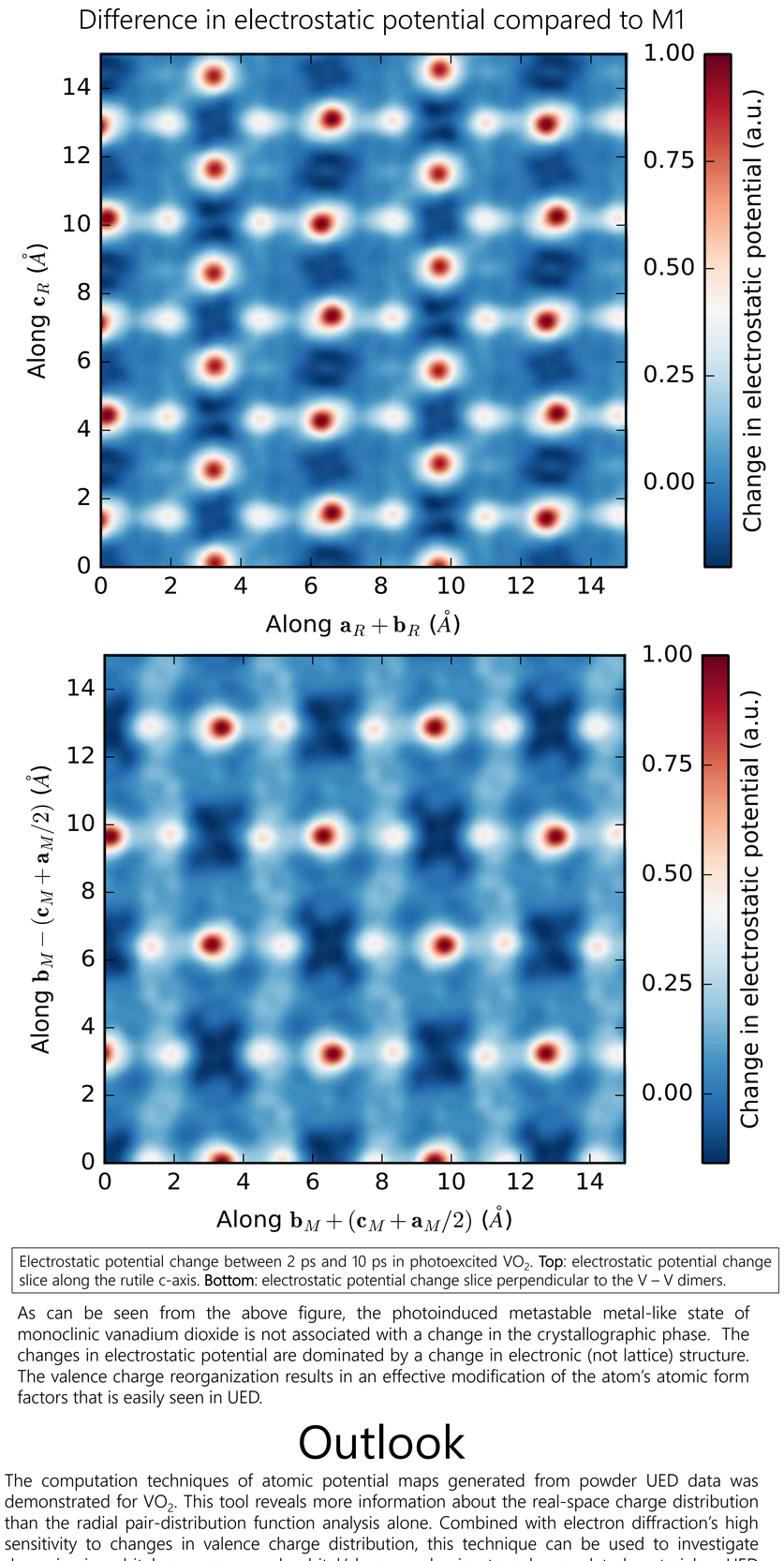

Electrostatic potential change between 2 ps and 10 ps in photoexcited VO_2. **Top**: electrostatic potential change slice along the rutile c-axis. **Bottom**: electrostatic potential change slice perpendicular to the V – V dimers.

As can be seen from the above figure, the photoinduced metastable metal-like state of monoclinic vanadium dioxide is not associated with a change in the crystallographic phase. The changes in electrostatic potential are dominated by a change in electronic (not lattice) structure. The valence charge reorganization results in an effective modification of the atom's atomic form factors that is easily seen in UED.

Outlook

The computation techniques of atomic potential maps generated from powder UED data was demonstrated for VO_2. This tool reveals more information about the real-space charge distribution than the radial pair-distribution function analysis alone. Combined with electron diffraction's high sensitivity to changes in valence charge distribution, this technique can be used to investigate dynamics in orbital occupancy and orbital/charge order in strongly correlated materials. UED should be seen as a powerful probe of electronic structure, not only lattice structure in condensed matter.

The computation of potential maps can be generalized to non-centrosymmetric crystals, (provided that the interrogated structure is known) and other scattering probes.

Acknowledgements

The code used for all computations presented on this poster is built on top of the open-source Scientific Python stack. All code used to make this poster is available either on our website www.physics.mcgill.ca/siwicklab/software.html or on demand.

The authors would like to thank group members Jean-Philippe Boisvert, Martin R. Otto and Mark J. Stern for their insight and for fruitful discussions. This work was supported by the following entities:

Fonds de recherche Nature et technologies Québec
NSERC CRSNG
INNOVATION.CA
CANADA FOUNDATION FOR INNOVATION | FONDATION CANADIENNE POUR L'INNOVATION

This research was undertaken, in part, thanks to funding from the Canada Research Chairs program.

References

[1] Morrison *et al.* (2014). *A photoinduced metal-like phase of monoclinic VO_2 revealed by ultrafast electron diffraction*. Science **346**, pp. 445 – 448.

[2] Chatelain *et al.* (2012). *Ultrafast Electron Diffraction with Radio-frequency Compressed Electron Pulses.* Appl. Phys. Lett. **101**, 081901.

[3] W. I. F. David, K. Shankland, L. B. McCusker and Ch. Baerlocher. *Structure Determination from Powder Diffraction Data*. Oxford Science Publications, New York, 2002.

[4] L. P. Rene de Cotret and B. J. Siwick (2017). *A general method for baseline-removal in ultrafast electron powder diffraction data using the dual-tree complex wavelet transform*. Struct. Dyn. **4**, 044004.